Journal of Materials Chemistry

www.rsc.org/materials

Volume 18 | Number 37 | 7 October 2008 | Pages 4353–4484

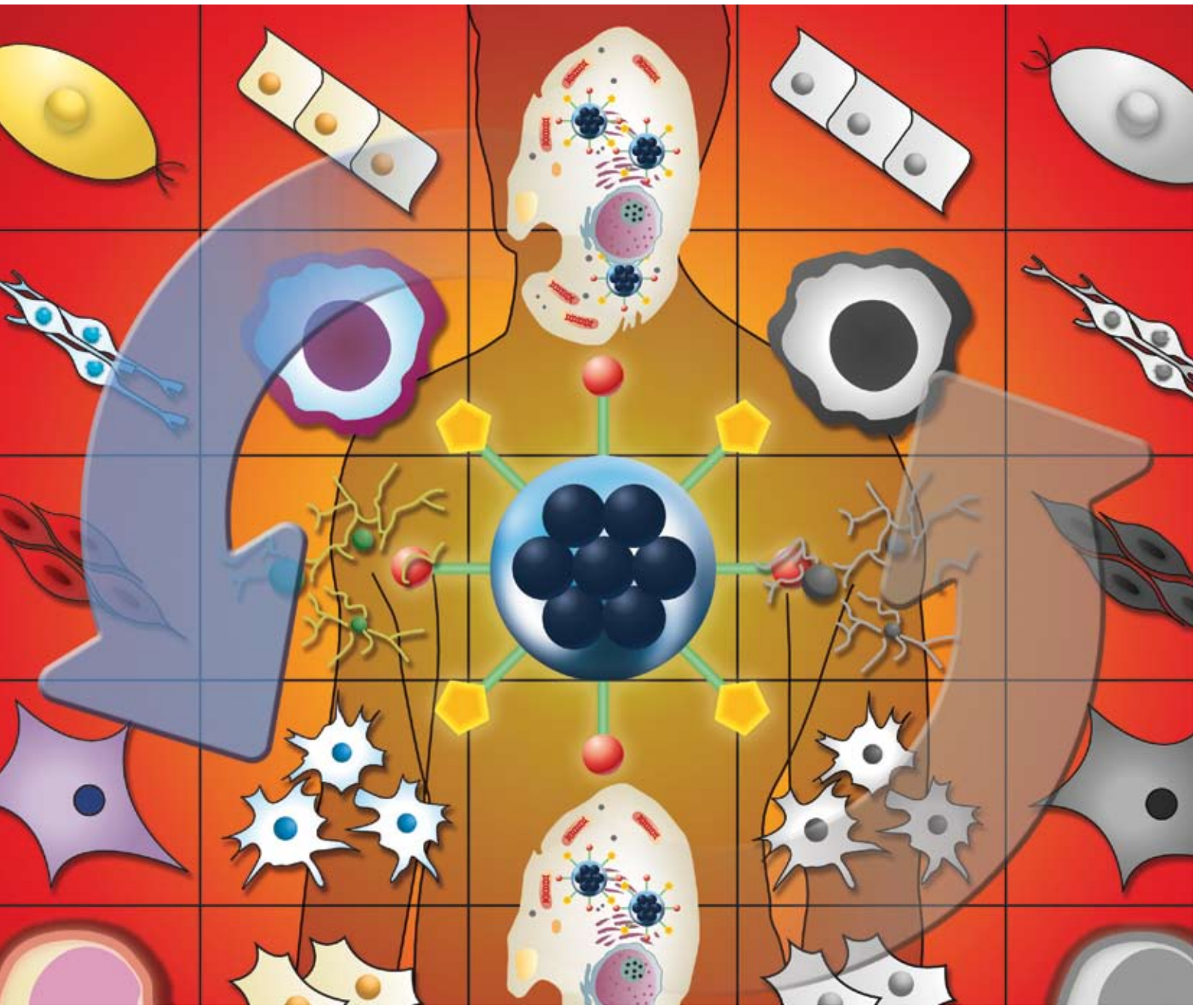

ISSN 0959-9428

PAPER
Seungjoo Haam *et al.*
Nanohybrids *via* a polycation-based nanoemulsion method for dual-mode detection of human mesenchymal stem cells

FEATURE ARTICLE
Robert Metzger
Unimolecular electronics

RSC Publishing

0959-9428(2008)18:37;1-Q

Nanohybrids *via* a polycation-based nanoemulsion method for dual-mode detection of human mesenchymal stem cells†

Sung-Baek Seo,[ab] Jaemoon Yang,[ab] Eun-Sook Lee,[c] Yukyung Jung,[ab] Kyujung Kim,[ad] Sang-Yup Lee,[b] Donghyun Kim,[ad] Jin-Suck Suh,[ac] Yong-Min Huh*[ac] and Seungjoo Haam*[ab]

Received 19th March 2008, Accepted 23rd May 2008
First published as an Advance Article on the web 3rd July 2008
DOI: 10.1039/b804544e

Fluorescent polycation-coated magnetic nanohybrids (FPMNs) were synthesized for the marking of human mesenchymal stem cells (hMSCs) and non-invasive tracking by both magnetic resonance (MR) and optical imaging. FPMNs were prepared by a polycation-based nanoemulsion method using magnetic nanocrystals (MNCs) as MR probes and polycationic polyethylenimine (PEI) which not only enhanced the affinity for hMSCs but also increased colloidal stability in the aqueous phase. Polycation-coated magnetic nanohybrids (PMNs) were further conjugated with a fluorescent dye (fluorescein isothiocyanate) to serve as optical imaging agents. FPMNs exhibited excellent colloidal stability and biocompatibility as well as high affinity for hMSCs. MR and optical images of hMSCs treated with FPMNs clearly demonstrated abundant potential as brilliant dual-mode imaging agents.

1. Introduction

Non-invasive monitoring of exogenous cells in the animal model has become a key issue in developing a successful regeneration system. Target cells are generally labeled using transfectable genes, magnetic nanoparticles, and fluorescent dye for visualizing histochemical procedures *via* positron emission tomography (PET), magnetic resonance (MR) and optical imaging.[1–6] Of all possible imaging modalities, MR imaging has been considered highly efficient for investigating the biodistribution of stem cells after labeling with magnetic substances because versatile and non-invasive MR imaging (MRI) allows excellent spatial resolution and contrast mechanisms providing both metabolic and structural information.[7,8] Although native magnetic nanocrystals (MNCs) currently appear to be the preferred cell-labeling agents,[9] they suffer from low labeling efficiency because MR imaging requires the target cells to be internally labeled with contrast agents. Hence, more efficient cellular-internalized labeling methods are highly desirable to acquire more detailed information from MR imaging. Several modifications of MNCs, *i.e.* coating with polystyrene, dextran, and dendrimers or utilizing other transfection agents, have been reported to improve cellular-internalization of the contrast agent.[10–12]

As an imaging tool for stem cell tracking, optical imaging is an emerging method that can benefit from a multimodal imaging strategy. This method is highly sensitive with the capability of detecting minute amounts of light emitting materials in a heterogeneous medium.[13,14] Moreover, fluorescence labeling of biomacromolecules and cells has also become one of the major tools for the study of structural organization, intra- and intermolecular processes within biological systems. Indeed, green fluorescent proteins (GFPs), small molecular polymethines and quantum dots (QDs) are widely employed as fluorescent tags.[15] We now recognize that MR and fluorescent imaging probes as stem cell tracking markers could colocalize to specific sites allowing simultaneous dual-mode detection. This enables us to provide unique and complementary information that improves the accuracy of stem cell tracking compared with that of single-mode detection using either magnetically or fluorescence labeled stem cells.

Herein, we report the synthesis of fluorescent polycation-coated magnetic nanohybrids (FPMNs) for dual-mode detection of human mesenchymal stem cells (hMSCs) *via* MR and optical imaging simultaneously *in vitro* at the cellular level. Thus, polycation-coated magnetic nanohybrids (PMNs) were prepared by a polycation-based nanoemulsion method using MNCs as MR probes and polycationic polyethylenimine (PEI) as a stabilizer without additional amphiphilic polymers (*i.e.*, polyvinyl alcohol or Pluronic series). Because PEI contains abundant amine groups, PMNs can be easily surface functionalized for bioconjugation procedures useful in many biological applications.[16–18] PMNs were further conjugated with fluorescein isothiocyanate (FITC) as optical imaging agents to formulate FPMNs. Fig. 1 shows the conceptual scheme for preparation of FPMNs. To assess their potential as markers and cell tracking agents, we evaluated the physicochemical properties of the FPMNs. Moreover, the cellular affinity and imaging efficiency of FPMNs for hMSCs have been extensively investigated using MR and optical imaging as well as cell viability tests.

[a]*Yonsei Nanomedical National Core Research Center, Seoul 120-749, South Korea*
[b]*Department of Chemical and Biomolecular Engineering, Yonsei University, Seoul 120-749, South Korea; Fax: +82-2-312-6401; Tel: +82-2-2123-2751*
[c]*Department of Radiology, College of Medicine, Yonsei University, Seoul 120-752, South Korea*
[d]*School of Electrical and Electronic Engineering, Yonsei University, Seoul 120-749, South Korea*

† Electronic supplementary information (ESI) available: Chemical constitution of PMNs, chemical quantification of FITC in FPMNs and colloidal stability studies of FPMNs. See DOI: 10.1039/b804544e

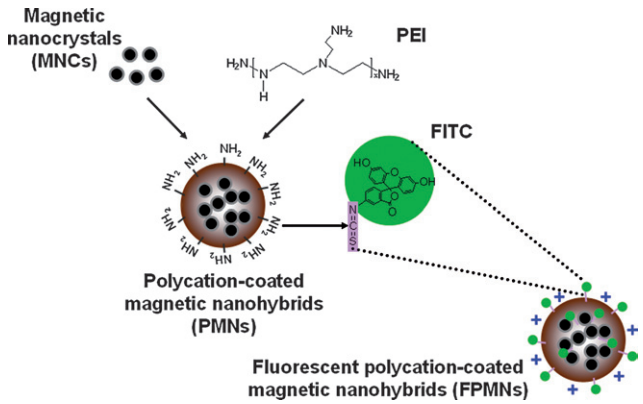

Fig. 1 A conceptual illustration of FPMNs as human mesenchymal stem cell (hMSC) markers for dual-mode detection *via* MR and optical imaging.

2. Experimental

2.1. Materials

Iron(III) acetylacetonate, manganese(II) acetylacetonate, 1,2-hexadecanediol, dodecanoic acid, dodecylamine, benzyl ether and polyethylenimine (PEI, M_w: 25 000 Da) were purchased from Sigma-Aldrich. Fluorescein isothiocyanate (FITC) was obtained from Fluka. Phosphate buffered saline (PBS; 10 mM, pH 7.4), and all culture media were purchased from Gibco. All other chemicals and reagents were of analytical grade.

2.2. Synthesis of magnetic nanocrystals (MNCs)

Magnetic nanocrystals (MNCs; $MnFe_2O_4$) were synthesized by thermal decomposition.[19] For the synthesis, 2 mmol of iron(III) acetylacetonate, 1 mmol of manganese(II) acetylacetonate, 10 mmol of 1,2-hexadecanediol, 6 mmol of dodecanoic acid, 6 mmol of dodecylamine and benzyl ether (20 mL) were mixed in a nitrogenous atmosphere. The mixture was pre-heated to 150 °C for 30 min and then refluxed at 300 °C for 30 min. After cooling to room temperature, the products were purified with an excess of pure ethanol.

2.3. Preparation of polycation-coated magnetic nanohybrids (PMNs)

Hydrophilic magnetic nanohybrids were formulated by the polycation-based nanoemulsion method. 20 mg of MNCs were dissolved in hexane (4 mL), and then added to PBS (20 mL) containing 50 mg of PEI. After mutual saturation of the organic and the continuous phase, the mixture was emulsified for 10 min under ultrasonication (ULH700S, Ulssohitech) at 420 W.[20] After solvent evaporation, the polycation-coated magnetic nanohybrids (PMNs) were purified by triple centrifugation at 15 000 rpm and stored under vacuum conditions.

2.4. Colloidal stability of PMNs

The colloidal stability of the prepared PMNs was determined from their resistance to sodium chloride and pH-induced aggregation. Specifically, 1 mL of nanoparticle suspension (13 mg mL^{-1}) was added to 3 mL of sodium chloride solution at various pHs (5–10) and concentrations (0–1.0 M) at room temperature, respectively. After mixing for 24 h, the size distribution of the suspension was measured using laser scattering.

2.5. Preparation of fluorescent polycation-coated magnetic nanohybrids (FPMNs)

FPMNs were synthesized by conjugation of FITC (0.58 mg mL^{-1}) with PEI (3.64 mg mL^{-1}) on the surface of PMNs (13 mg mL^{-1}) at room temperature for 12 h in a darkroom. The isothiocyanate group of FITC is exceedingly reactive towards the amine group of PEI.[21] The resulting products were purified by triple centrifugation at 6800 rpm using a centrifugal filter (MWCO 1000, Amicon Ultra-15, Millipore).

2.6. Characterizations

The morphologies of MNCs and PMNs were evaluated with a transmission electron microscope (TEM, JEM-1011, JEOL Ltd), and size distribution and surface charges of PMNs and FPMNs were measured by laser scattering (ELS-Z, Otsuka electronics). FT-IR spectra (Excalibur™ series, Varian Inc.) analysis was performed to confirm the characteristic bands of the synthesized FPMNs. The presence of conjugated FITC in PBS was detected by a UV-vis spectrophotometer (Optizen 2120UV, MECASYS Co.). The saturation of magnetization was evaluated using a vibrating-sample magnetometer (VSM, MODEL-7300, Lakeshore). The ionic amounts of FPMNs were determined by inductively coupled plasma mass spectrometry (ICP-MS, Elan 6100, Perkin Elmer).

2.7. Cytotoxicity studies

Cytotoxicity of FPMNs for bone-marrow-derived human mesenchymal stem cells (hMSCs) was determined by MTT assay using a cell proliferation kit (Roche, Germany). Briefly, hMSCs (1×10^5 cells mL^{-1}) were placed in a 96-microwell plate overnight at 37 °C. hMSCs were then treated with various concentrations (0.8–400 μg mL^{-1}) of PMNs and FPMNs, respectively. The plate was incubated overnight at 37 °C and the optical density of the wells was determined using a microplate reader (ELISA, Enzyme-Linked ImmunoSorbent Assay, BioTek®, UK) at a test wavelength of 570 nm and a reference wavelength of 690 nm. All experiments were performed in triplicate. The control cells were grown under the same conditions without the addition of PMNs and FPMNs. Cell viabilities were calculated using non-treated control cells.

2.8. Cell affinity test

A culture medium containing PMNs or FPMNs was added to hMSCs for labeling in 75 cm^2 flasks, respectively. The final iron concentration for labeling hMSCs (20 μg mL^{-1}) was pre-determined from the previous tests.[22] The cell cultures were kept at 37 °C for 12 h in an incubator containing 95% air and 5% CO_2. After incubation, the hMSCs were washed three times with PBS to remove unreacted PMNs and FPMNs and 4′,6-diamidino-2-phenylindole (DAPI) was used to stain the nuclei of hMSCs for fluorescence microscopic imaging. Fluorescence images for

hMSCs labeled by PMNs or FPMNs were visualized by an epi-fluorescence microscope (EFM 510, Olympus, Tokyo, Japan), respectively. Otherwise, cellular uptake efficiencies of PMNs and FPMNs were also examined by the Prussian blue staining method, respectively. For staining of magnetic components in hMSCs labeled by PMNs or FPMNs, specifically, the cells were incubated with 2% potassium ferrocyanide in 10% hydrochloric acid and then counterstained for the outlines of cells and magnetic substances, respectively.

2.9. MR imaging procedure

MR imaging experiments were performed with a 1.5 T clinical MR imaging instrument with a micro-47 surface coil (Intera, Philips Medical Systems). T2-weighted images (T2 = spin–spin relaxation time) for PMNs and FPMNs containing MNCs were investigated at room temperature using the Carr–Purcell–Meiboom–Gill (CPMG) sequence: time of repetition (TR) = 10 s, 32 echoes with 12 ms, even echo space, number of acquisitions = 1, a point resolution of 156 × 156 μm, and a section thickness of 0.6 mm. The relative T2 values (%) equal the ratio of T2 in hMSCs treated with PMNs or FPMNs to the T2 in non-treated hMSCs.

2.10. Optical imaging procedure

Optical imaging experiments were performed with a pre-clinical optical molecular imager, eXplore Optix™ (G.E. Medical Systems), fitted with a pulsed laser operating at 470 nm and a filtered diode detector at 520 nm. hMSCs treated with PMNs and FPMNs in the plate were placed in the heated base (36.5 °C) of the imaging system. The optimal elevation of the solutions and cells was verified *via* a side-viewing digital camera. Laser power and counting time per pixel were optimized at 20 mW and 1.0 s, respectively. These values remained constant during the entire experiment. The raster scan interval was 0.5 mm and was held constant during the acquisition of each frame. The data were processed by OptiView software. The fluorescence intensity (a. u.) was calculated by the ratio of photon counts in hMSCs treated with PMNs or FPMNs to the photon counts in non-treated hMSCs.

2.11. Statistical analysis

All experiments were performed in triplicate, and the values are expressed as an average ± standard deviation. The statistical evaluation of data was performed by analysis of variance (ANOVA), followed by Tukey's test for comparison of cell viability, T2 and fluorescence intensity from different groups. $p < 0.05$ was considered to be statistically significant.

3. Results and discussion

Magnetic nanocrystals (MNCs, $MnFe_2O_4$) were synthesized by thermal decomposition as MR imaging agents. The spherical morphology and high monodispersity of MNCs in hexane were evaluated by TEM (Fig. 2a). MNCs were only soluble in organic solvents (Fig. 2a, inset) because they were coated with a hydrophobic ligand (dodecanoic acid).[23] In order to use MNCs as biomedical probes, it is necessary to modify their surface with a hydrophilic moiety to promote solubility in an aqueous media. For this purpose, polyethylenimine (PEI) was introduced to cover the surface of MNCs using a nanoemulsion method, to fabricate PEI-coated magnetic nanohybrids by the following routes: (i) creating emulsion droplets containing MNCs in aqueous solution by sonication, (ii) enclosing emulsion droplets by PEI, (iii) coating of polycationic PEI around MNCs during solvent evaporation and then (iv) formation of hydrogen bonds between the nitrogen of PEI and the hydrogen of water molecules. Herein, polycationic PEI can enhance the cellular affinity and the uptake efficiency by associating with negatively charged cell membranes.[24,25] Fig. 2b demonstrates that PMNs were well-dispersed in the aqueous phase and PEI effectively incorporated MNCs. The narrow size distribution (74.0 ± 4.2 nm) of PMNs was confirmed by laser scattering. To evaluate the magnetic sensitivity of MNCs and PMNs under a magnetic field, the magnetic moment was analyzed using a vibrating-sample magnetometer (VSM). The magnetic hysteresis loop of both MNCs and PMNs at room temperature exhibited superparamagnetic behavior without magnetic hysteresis (Fig. 2c). The saturation of magnetization values of MNCs and PMNs at 0.9 T were 56.3 and 38.2 emu g^{-1}, respectively. The saturation of magnetization value of the PMNs was lower than that of MNCs due to the presence of organic PEI compounds.

As shown in Fig. 3a and b, we observed the colloidal stability of PMNs over a wide range of pHs (5–10) and at various sodium chloride (NaCl) concentrations (0–1.0 M), respectively. PMNs continuously maintained stable conditions even after 1 month because positively charged PMNs (around 20 mV) were stabilized in the aqueous phase by electrostatic repulsion.[26] The particle size and ζ potential of PMNs in PBS were plotted against

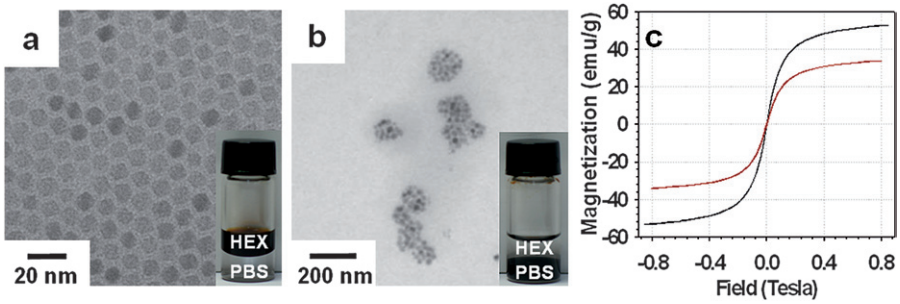

Fig. 2 TEM images and solubility tests (inset) of (a) MNCs in hexane, (b) PMNs in phosphate buffered saline (PBS; 10 mM, pH 7.4) and (c) magnetic hysteresis loops for MNCs (black line) and PMNs (brown line).

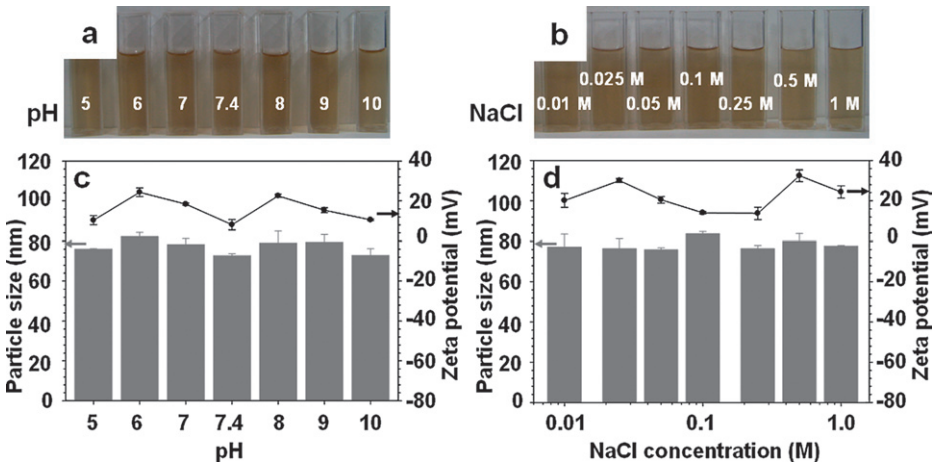

Fig. 3 Photographs of PMNs solutions under various (a) pH conditions and (b) NaCl concentrations. Particle size and ζ potential of PMNs plotted against various (c) pH conditions and (d) NaCl concentrations.

various pH conditions and concentrations of NaCl using laser scattering (Fig. 3c and d). PMNs exhibited uniform particle size and stable ζ potential values without aggregation under these conditions.

To be utilized as optical imaging agents as well as MR imaging probes, fluorescent polycation-coated magnetic nanohybrids (FPMNs) were synthesized by conjugation between primary amine ($-NH_2$) groups on the surface of PMNs and the isothiocyanate (–N=C=S) groups of FITC. The carbon atom in the isothiocyanate group was attacked by electrons of the nitrogen atom in the amine group as a nucleophile.[21] In Fig. 4a, FT-IR spectra were used to evaluate the chemical structures of PMNs and FPMNs. The characteristic peak of PEI in PMNs was observed at 1600 cm^{-1} due to the primary amine group. Furthermore, the characteristic peak of the Fe–O band in MNCs was observed at 585 cm^{-1}. The isothiocyanate (–N=C=S) group of FITC was confirmed at 2125 cm^{-1}. During the preparation of FPMNs, the characteristic peak of PEI was not altered and a new isothiocanate (–N=C=S–H–) group of FPMNs was presented at 1350 cm^{-1}. These results indicated that MNCs existed successfully in PMNs and that FITC was well conjugated on the surface of PMNs. To further confirm the presence of FITC in FPMNs, UV-vis absorption spectroscopy was performed. The characteristic bands of MNCs in PMNs and FITC were observed at 245 nm and 492 nm, respectively. The characteristic bands of FPMNs are shown in Fig. 4b.

Moreover, the ζ potentials of PMNs and FPMNs in PBS were 20.0 ± 3.4 and 14.6 ± 2.5 mV, respectively. This decreased ζ potential value from PMNs to FPMNs showed that the numbers of protonated amine groups in FPMNs were fewer than those in PMNs due to the chemical conjugation between the primary amine ($-NH_2$) group of PMNs and the isothiocyanate (–N=C=S) group of the FITC.

We next determined the *in vitro* cytotoxic effect measured by MTT assay to assess whether PMNs and FPMNs had any deleterious biological properties, and the results are shown in Fig. 5. The cell viability of PMNs and FPMNs retained over 80% for the concentration range of 0.8–100 μg mL^{-1}, which means that the prepared nanohybrids were biocompatible.

To evaluate the labeling efficiency of FPMNs as hMSCs tracking markers *via* dual-mode detection, the fluorescence microscopy images of hMSCs treated with FPMNs were compared to those of non-treated hMSCs and hMSCs treated with PMN. First, to investigate magnetic labeling efficiency with FPMNs, Prussian blue stained hMSCs were observed in Fig. 6a–c. The red color indicates hMSCs, and the blue color represents iron (Fe). hMSCs treated with PMNs or FPMNs clearly exhibited the presence of MNCs when compared to the non-treated hMSCs. This result demonstrates that Prussian blue staining of hMSCs treated with FPMNs shows a high degree of

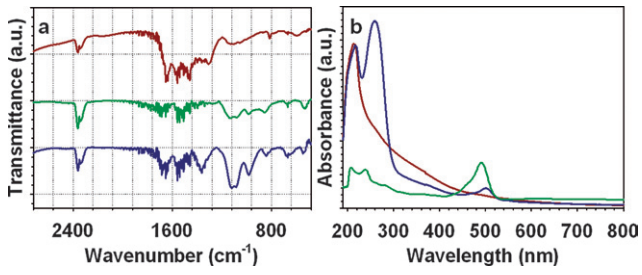

Fig. 4 (a) FT-IR spectra of PMNs (brown line), FITC (green line) and FPMNs (blue line), (b) UV-Vis absorption spectra of PMNs (brown line), FITC (green line), and (c) FPMNs (blue line) in PBS.

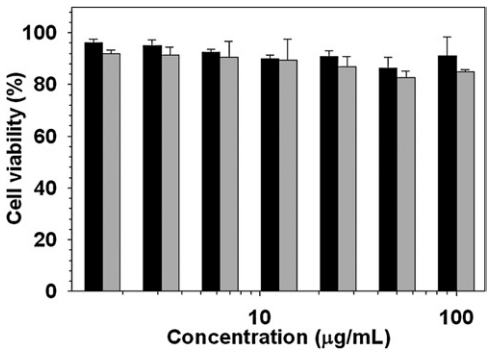

Fig. 5 The cell viability test of hMSCs by MTT assay for cells treated with PMNs (black bar) and FPMNs (gray bar) at various concentrations.

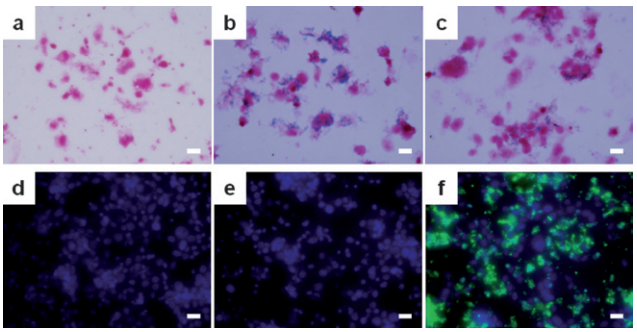

Fig. 6 Microscopy images of Prussian blue stained hMSCs; (a) non-treated, (b) treated with PMNs, (c) treated with FPMNs. Epi-fluorescence microscopy images of (d) non-treated hMSCs, (e) hMSCs treated with PMNs and (f) hMSCs treated with FPMNs; green: FITC and blue: DAPI. Scale bars: 10 μm.

labeling and potential utility as a hMSCs tracking marker for MR imaging.

Furthermore, it was obvious that hMSCs treated with FPMNs generated strong fluorescence due to the conjugated FITCs of FPMNs (Fig. 6f), while no fluorescence existed in non-treated hMSCs or hMSCs treated with PMNs (Fig. 6d and e). The blue color indicates the nuclei of hMSCs by DAPI staining. The result apparently indicates that FPMNs exhibited hMSCs tracking markers *via* optical imaging.

We also investigated MR and optical contrast efficacies of FPMNs for hMSCs. The changes of T2-weighted MR intensity and fluorescence intensity in hMSCs indicate the potential for dual-mode detection. First, the T2-weighted MR images of hMSCs treated with PMN or FPMN presented a darker black color than that of non-treated hMSCs (Fig. 7a). These results

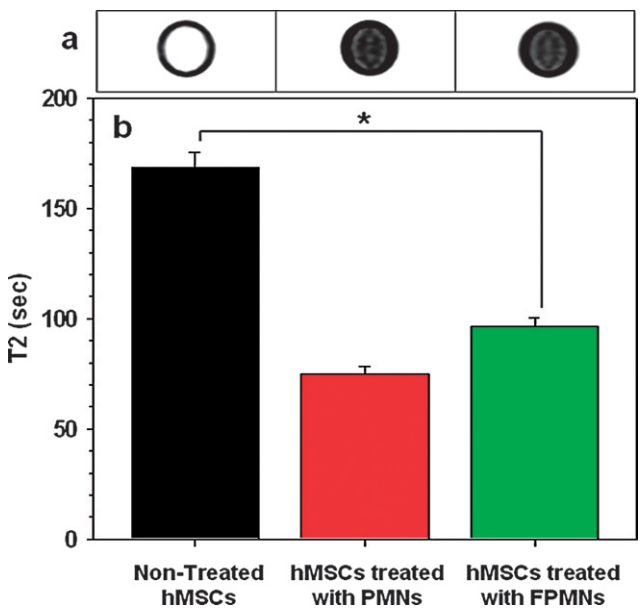

Fig. 7 (a) T2-weighted MR images (non-treated hMSCs, left; hMSCs treated with PMNs, center; and hMSCs treated with FPMNs, right) and (b) T2 graph for hMSCs. Statistical significance was performed by ANOVA followed by Tukey's test (*, $p<0.05$ non-treated hMSCs *vs.* hMSCs treated with FPMNs).

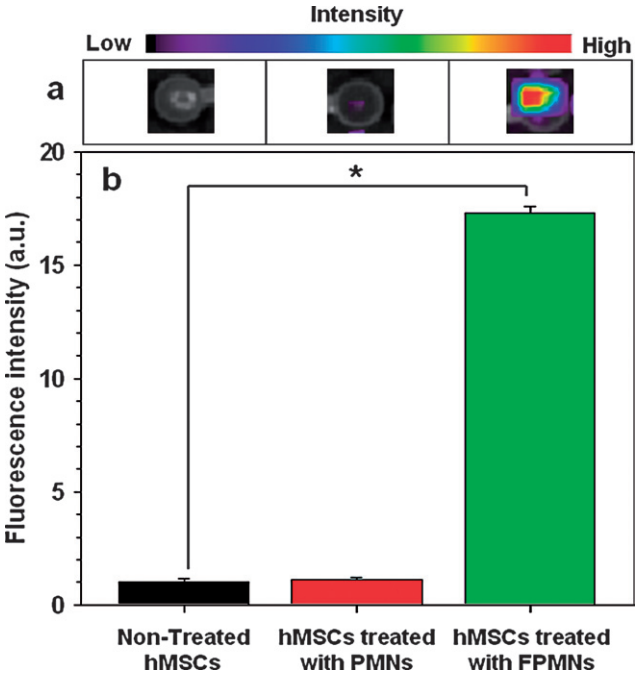

Fig. 8 (a) Optical images (non-treated hMSCs, left; hMSCs treated with PMNs, center; and hMSCs treated with FPMNs, right) and (b) fluorescence intensity graph for hMSCs. Statistical significance was performed by ANOVA, followed by Tukey's test (*, $p<0.05$ non-treated hMSCs *vs.* hMSCs treated with FPMNs).

demonstrated that hMSCs treated with PMN or FPMN exhibited excellent cellular uptake efficiency due to the electrostatic interaction between polycationic nanohybrids and the anionic membrane of hMSCs. In particular, the relative T2 value of FPMNs treated hMSCs (57.2 ± 4.0%) exhibited sufficient cellular uptake efficiency, even though the ζ potential value of FPMNs slightly decreased from that of PMNs. These noteworthy results indicate that cationic FPMNs not only exhibit efficient MR imaging agents but also increase affinity to hMSCs.

On the other hand, the optical images and the fluorescence intensity of non-treated hMSCs and hMSCs treated with PMN or FPMN is shown in Fig. 8. The optical image of hMSCs treated with FPMNs exhibited excellent signal intensity compared to non-treated and hMSCs treated with PMNs (Fig. 8a). As shown in Fig. 8b, the fluorescence intensity of the hMSCs treated with FPMNs was approximately 17 times higher than that of the non-treated cells. These results demonstrate that FPMNs show sufficient potential as hMSCs tracking markers *via* optical imaging. Consequently, FPMNs demonstrate adequate ability for hMSCs tracking markers *via* dual-mode detection in MR and optical imaging.

Conclusions

We successfully synthesized fluorescent polycation-coated magnetic nanohybrids (FPMNs) for human mesenchymal stem cells (hMSCs) tracking markers and dual-mode detection. Polycation-coated magnetic nanohybrids (PMNs) were composed of magnetic nanocrystals (MNCs) and polycationic PEI. Water-soluble PMNs were sucessfully prepared by

a polycation-based nanoemulsion method using only hydrophilic compartments. Polycationic PEI on the surface of PMNs could be conjugated with fluorescence dye (FITC) and enhance colloidal stability. Moreover, biocompatibility and a high order of hMSCs affinity of FPMNs were also investigated. Therefore, FPMNs demonstrated unlimited potential as hMSCs tracking agents *via* MR and optical imaging.

Acknowledgements

This work was supported by the Korea Science and Engineering Foundation (KOSEF) (R15-2004-024-00000-0, M10755020001-07N5502-00110, R01-2006-000-10023-0 and 2007-04717), by Korea Research Foundation Grant (KRF-2005-005-J01401) and a grant from the National R&D Program for Cancer Control, Korean Ministry of Health and Welfare (0620190-1).

References

1 J. V. Frangioni and R. J. Hajjar, *Circulation*, 2004, **110**, 3378.
2 J. C. Wu, I. Y. Chen, G. Sundaresan, J.-J. Min, A. De, J.-H. Qiao, M. C. Fishbein and S. S. Gambhir, *Circulation*, 2003, **108**, 1302.
3 B. B. Chin, Y. Nakamoto, J. W. Bulte, M. F. Pittenqer, R. Wahl and D. L. Kraitchman, *Nucl. Med. Commun.*, 2003, **24**, 1149.
4 W. S. Seo, J. H. Lee, X. Sun, Y. Suzuki, D. Mann, Z. Liu, M. Terashima, P. C. Yang, M. V. McConnell, D. G. Nishimura and H. Dai, *Nat. Mater.*, 2006, **5**, 971.
5 C. Wu, D. Tian, Y. Feng, P. Polak, J. Wei, A. Sharp, B. Stankoff, C. Lubetzki, B. Zalc, E. J. Mufson, R. M. Gould, D. L. Feinstein and Y. Wang, *J. Histochem. Cytochem.*, 2006, **54**, 997.
6 L. Josephson, C. H. Tung, A. Moore and R. Weissleder, *Bioconjugate Chem.*, 1999, **10**, 186.
7 M. Lewin, N. Carlesso, C. H. Tung, X. W. Tang, D. Cory, D. T. Scadden and R. Weissleder, *Nat. Biotechnol.*, 2000, **18**, 410.
8 H. E. Daldrup-Link, M. Rudelius, G. Piontek, S. Metz, R. Brauer, G. Debus, C. Corot, J. Schlegel, T. M. Link, C. Peschel, E. J. Rummeny and R. A. Oostendorp, *Radiology*, 2005, **234**, 197.
9 J. W. Bulte and D. L. Kraitchman, *NMR Biomed.*, 2004, **17**, 484.
10 J. M. Hill, A. J. Dick, V. K. Raman, R. B. Thompson, Z. X. Yu, K. A. Hinds, B. S. Pessanha, M. A. Guttman, T. R. Varney, B. J. Martin, C. E. Dunbar, E. R. McVeigh and R. J. Lederman, *Circulation*, 2003, **108**, 1009.
11 P. Jendelova, V. Herynek, J. DeCroos, K. Glogarova, B. Andersson, M. Hajek and E. Sykova, *Magn. Reson. Med.*, 2003, **50**, 767.
12 S. Ju, G. Teng, Y. Zhang, M. Ma, F. Chen and Y. Ni, *Magn. Reson. Imaging*, 2006, **24**, 611.
13 X. Wang, M. Rosol, S. Ge, D. Peterson, G. McNamara, H. Pollack, D. B. Kohn, M. D. Nelson and G. M. Crooks, *Blood*, 2003, **102**, 3478.
14 Y.-A. Cao, A. J. Wagers, A. Beilhack, J. Dusich, M. H. Bachmann, R. S. Negrin, I. L. Weissman and C. H. Contag, *Proc. Natl. Acad. Sci. U. S. A.*, 2004, **101**, 221.
15 J. V. Frangioni, *Curr. Opin. Chem. Biol.*, 2003, **7**, 626.
16 S. C. McBain, H. H. P. Yiu, A. El Haj and J. Dobson, *J. Mater. Chem.*, 2007, **17**, 2561.
17 A. F. Thunemann, D. Schutt, L. Kaufner, U. Pison and H. Mohwald, *Langmuir*, 2006, **22**, 2351.
18 S. Francisa, L. Varshneya and K. Tirumalesh, *Radiat. Phys. Chem.*, 2006, **75**, 747.
19 J.-H. Lee, Y.-M. Huh, Y. Jun, J. Seo, J. Jang, H.-T. Song, S. Kim, E.-J. Cho, H.-G. Yoon, J.-S. Suh and J. Cheon, *Nat. Med.*, 2007, **13**, 95.
20 S.-B. Seo, J. Yang, W. Hyung, E.-J. Cho, T.-I. Lee, Y. J. Song, H.-G. Yoon, J.-S. Suh, Y.-M. Huh and S. Haam, *Nanotechnology*, 2007, **18**, 475105.
21 J. H. Jeong, S. W. Kim and T. G. Park, *J. Controlled Release*, 2003, **93**, 183.
22 Y.-M. Huh, E.-S. Lee, J.-H. Lee, Y. Jun, P.-H. Kim, C.-O. Yun, J.-H. Kim, J.-S. Suh and J. Cheon, *Adv. Mater.*, 2007, **19**, 3109.
23 J. Yang, T.-I. Lee, J. Lee, E.-K. Lim, W. Hyung, C.-H. Lee, Y. Song, J.-S. Suh, H.-G. Yoon, Y.-M. Huh and S. Haam, *Chem. Mater.*, 2007, **19**, 3870.
24 H. Song, J. Choi, Y. Huh, S. Kim, Y. Jun, J. Suh and J. Cheon, *J. Am. Chem. Soc.*, 2005, **127**, 9992.
25 A. Ito, E. Hibino, H. Honda, K. Hata, H. Kagamic, M. Uedad and T. Kobayashi, *Biochem. Eng. J.*, 2004, **20**, 119.
26 C.-W. Chen, C. S. Oakes, K. Byrappa, R. E. Riman, K. Brown, K. S. TenHuisen and V. F. Janas, *J. Mater. Chem.*, 2004, **14**, 2425.